Articles

A Density Functional Study of C_{60} Transition Metal Complexes

Francesca Nunzi and Antonio Sgamellotti*

Dipartimento di Chimica e Centro Studi CNR per il Calcolo Intensivo in Scienze Molecolari, Università di Perugia, I-06123 Perugia, Italy

Nazzareno Re

Facoltà di Farmacia, Università G. D'Annunzio, I-66100 Chieti, Italy

Carlo Floriani

Institut de Chimie Minérale et Analytique, University of Lausanne, CH-1015 Lausanne, Switzerland

Received October 22, 1999

Density functional calculations have been performed on $(PH_3)_2M(\eta^2\text{-}C_{60})$ (M = Ni, Pd, Pt) complexes. The optimized geometries have been found in good agreement with the X-ray experimental data. The electronic structure has been analyzed in terms of the Chatt−Dewar−Duncanson model, and the contribution from π back-donation was found to dominate over that from σ donation for all three complexes. Reliable values for the metal fullerene bond dissociation energies have been calculated and found higher than the corresponding metal ethylene complexes, but lower than metal tetrafluoro- and tetracyanoethylene complexes.

1. Introduction

Since the first preparation of organometallic complexes of fullerene,[1,2] many transition metal fullerene complexes have been synthesized and structurally characterized.[3] Multiple addition is also possible, and a few dinuclear and hexanuclear fullerene complexes have been isolated.[1,4−7]

Although every carbon atom in C_{60} is chemically equivalent, two different types of C−C bonds can be distinguished, corresponding to the fusion of two six-membered rings, [6,6] bond, and of a six-membered and a five-membered ring, [6,5] bond.[8,9] In all the characterized transition metal fullerene complexes, C_{60} acts as an electron-deficient polyalkene and the metal atom is attached in a dihapto fashion to a [6,6] bond. Metal attaching causes a lengthening of the C−C bond with respect to free C_{60} of about 0.01−0.15 Å and a pulling out from the pseudospherical surface of the C−C edge. The degree of pullout may be indicated by the increase of the pyramidalization angle (defined as the angle between the C−*C* axis and the plane containing one of these carbon atoms and its two neighbor carbons in the fullerene cage; see Figure 1) with respect to the value observed for the free C_{60}. Most of the synthesized complexes are based on electron-rich transition metals, such as those of group VIII. In particular, several $(PR_3)_2M(\eta^2\text{-}C_{60})$ complexes of the Ni, Pd, Pt triad with

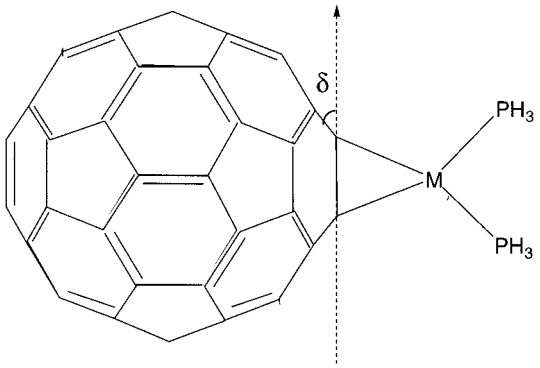

Figure 1. Geometry of $(PH_3)_2M(\eta^2\text{-}C_{60})$ complexes, M = Ni, Pd, Pt.

(1) Fagan, P. J.; Calabrese, J. C.; Malone, B. *Acc. Chem. Res.* **1997**, *25*, 134.
(2) Hawkins, J. M. *Acc. Chem. Res.* **1992**, *25*, 150.
(3) Stephens, A. H. H.; Green, M. L. H. *Adv. Inorg. Chem.* **1997**, *44*, 1.
(4) Fagan, P. J.; Calabrese, J. C.; Malone, B. *Science* **1991**, *252*, 1160.
(5) Fagan, P. J.; Calabrese, J. C.; Malone, B. *J. Am. Chem. Soc.* **1991**, *113*, 9408.
(6) Hawkins, J. M.; Meyer, A.; Lewis, T. A.; Bunz, U.; Nunlist, R.; Ball, G. E.; Ebessen, T. W.; Tanigaki, K. J. *J. Am. Chem. Soc.* **1992**, *114*, 7954.
(7) Balch, A. L.; Lee, J. W.; Noll, B. C.; Olmstead, M. M. *J. Am. Chem. Soc.* **1992**, *114*, 10984.
(8) Hawkins, J. M.; Meyer, A.; Lewis, T. A.; Loren, S.; Hollander, F. J. *Science* **1991**, *252*, 312.
(9) (a) David, W. I. F.; Ibberson, R. M.; Matthewman, J. C.; Prassides, K.; Dennis, T. J. S.; Hare, P. J.; Kroto, H. W.; Taylor, R.; Walton, D. R. M. *Nature* **1991**, *252*, 1160. (b) Hedberg, K.; Hedberg, L.; Bethune, D. S.; Brown, C. A.; Dorn, H. C.; Johnson, R. D.; de Vries, M. *Science* **1991**, *254*, 410.

10.1021/om9908478 CCC: $19.00
Publication on Web 03/25/2000

R = Ph, Et have been synthesized and those of palladium and platinum structurally characterized.[4,10]

Accurate theoretical calculations on transition metal complexes of fullerene have been prevented by their size. Few theoretical investigations have been performed on these systems, mainly at the semiempirical level[1,3,10,11] and, to our knowledge, only two at the ab initio level.[13,14] Koga and Morokuma have reported a molecular orbital calculation on $(PH_3)_2Pt(\eta^2\text{-}C_{60})$ at the HF level with a relativistic ECP [3s,3p,3d] basis set on Pt and a 3-21G set on P, C, and H. Bo et al. reported analogous HF calculations on $(PH_3)_2Pd(\eta^2\text{-}C_{60})$, $(PH_3)_2Pt(\eta^2\text{-}C_{60})$, and their di- and hexa-substituted derivatives with double-ζ basis sets on P, C, and H and including a polarization function on P. Although the optimized geometries are in quite good agreement with the experimental X-ray data, the calculated bonding energies were strongly underestimated because of the neglect of electron correlation.

In this work we carry out an accurate theoretical study on the $(PH_3)_2M(\eta^2\text{-}C_{60})$ complexes for the group 10 metals Ni, Pd, and Pt at the DFT nonlocal level using double-ζ polarized basis sets for P, C, and H. The aim of this study is to investigate the electronic structure of these complexes, with special attention to the relative importance of σ donation and π back-donation, and to give reliable estimates for the interaction energy between fullerene and the metal fragment. Since C_{60} shows physical and chemical properties similar to those of electron-deficient alkenes, we compared the electronic structures of the considered fullerene complexes with those of ethylene and fluoro- and cyano-substituted ethylene which have been recently investigated.[15]

2. Computational Details

The calculations reported in this paper are based on the ADF (Amsterdam Density Functional) program package.[16] Its main characteristics are the use of a density fitting procedure to obtain accurate Coulomb and exchange potentials in each SCF cycle, the accurate and efficient numerical integration of the effective one-electron Hamiltonian matrix elements, and the possibility to freeze core orbitals. The molecular orbitals were expanded in an uncontracted double-ζ Slater-type orbital (STO) basis set for all main group atoms. For transition metal orbitals we used a double-ζ STO basis set for *n*s and *n*p and a triple-ζ STO basis set for *n*d and (*n*+1)s. As polarization functions, we used one (*n*+1)p function for transition metals, one 3d for P, C, N, and F, and one 2p for H. The inner shell cores have been kept frozen.

The LDA exchange correlation potential and energy were used, together with the Vosko−Wilk−Nusair parametrization[17] for homogeneous electron gas correlation, including Becke's nonlocal correction[18] to the local exchange expression and Perdew's nonlocal correction[19] to the local expression of correlation energy. Molecular structures of all considered complexes were optimized at this nonlocal (NL) level in C_{2v} symmetry.

Table 1. Optimized Geometries of $(PH_3)_2M(C_{60})$ Complexes (Bond Lengths in Angstroms and Bond Angles in Degrees)

molecule	$R_{([5,6])}$	$R_{([6,6])}$	$R_{(M-C)}$	$R_{(M-P)}$	∠PMP	δ
			Calculated			
$(PH_3)_2Ni(C_{60})$	1.474	1.470	1.989	2.222	113.0	39.3
$(PH_3)_2Pd(C_{60})$	1.471	1.464	2.180	2.378	111.0	38.8
$(PH_3)_2Pt(C_{60})$	1.485	1.505	2.103	2.289	107.4	41.8
			Experimental			
$(PPh_3)_2Pd(C_{60})$[a]	1.490	1.447	2.104	2.322	109.7	39.0
$(PPh_3)_2Pt(C_{60})$[b]		1.502	2.130	2.278	102.4	41.0

[a] Reference 10. [b] Reference 5.

3. Results and Discussion

Geometry Optimization. We first performed a geometry optimization on the free buckminsterfullerene molecule under D_{2h} symmetry constraints. The computed values of 1.392 and 1.447 Å respectively for the [6,6] and [6,5] bonds are very close to the experimental values of 1.391 and 1.455 Å from neutron powder diffraction[9a] and of 1.401 and 1.458 Å from electron diffraction.[9b] These computed values are close to the results of the previous highest level calculations, MP2 with triple-ζ plus polarization basis set (1.406 and 1.446 Å).[20]

All X-ray structures available for metal diphosphine fullerene complexes show the [6,6] C−C bond in the MP_2 plane rather than perpendicular to it, analogously to the situation observed for the corresponding ethylene complexes. All geometry optimizations on fullerene complexes were therefore performed in the parallel orientation with imposed C_{2v} symmetry constraints; see Figure 1. The preference for the parallel orientation has been checked in the $(PH_3)_2Ni(\eta^2\text{-}C_{60})$ complex, for which the perpendicular structure has been found 4.3 kJ mol^{-1} higher than the parallel one, in agreement with the experimental evidence.

The results of the geometry optimization of the $(PH_3)_2M(\eta^2\text{-}C_{60})$, M = Ni, Pd, Pt, complexes show a significant distortion of the C_{60} unit, mainly localized in the interaction region with a lengthening of the C−C bond directly bound to the metal fragment and its pullout from the fullerene pseudosurface. The computed parameters are compared in Table 1 with the available experimental values. A direct comparison between theoretical and experimental geometries is difficult, as most of the observed structures refer to aryl- or alkyl-substituted phosphines and multiply substituted fullerene. In particular, the experimental data in Table 1 refers to $(PPh_3)_2Pd(C_{60})$ and $(PPh_3)_2Pt(C_{60})$. The calculated values compare quite well with the available experimental data. Bond length deviations are within 0.08 Å and could, in part, be due to the use of model PH_3 ligands on the metal atoms, which are less electron releasing than the PPh_3 or PEt_3 ligands on the actual

(10) (a) Bashilov, V. V.; Petrovskii, P. V.; Sokolov, V. I.; Lindeman, S. V.; Guzey, I. A.; Struchkov, Y. T. *Organometallics* **1993**, *12*, 991. (b) Nagashima, H.; Yamaguchi, H.; Kato, Y.; Saito, Y.; Haga, M.; Itoh, K. *Chem. Lett.* **1993**, 2153.
(11) Lopez, J. A.; Mealli, C. *J. Organomet. Chem.* **1994**, *478*, 161.
(12) Fujimoto, H.; Nakao, Y.; Fukui, K. *J. Mol. Struct.* **1993**, *300*, 425.
(13) Koga, N.; Morokuma, K. *Chem. Phys. Lett.* **1993**, *202*, 330.
(14) Bo, C.; Costas M.; Poblet, J. M. *J. Phys. Chem.* **1995**, *99*, 5914.
(15) Nunzi, F.; Sgamellotti A.; Re N.; Floriani C. *J. Chem. Soc., Dalton Trans.* **1999**, 3487.
(16) Baerends, E. J.; Ellis, D. E.; Ros, P. *Chem. Phys.* **1973**, *2*, 42. Boerrigter, P. M.; Velde, G.; Baerends, E. J. *Int. J. Quantum Chem.* **1988**, *33*, 87.
(17) Vosko, S. H.; Wilk, L.; Nusair, M. *Can. J. Phys.* **1980**, *58*, 1200.
(18) Becke, A. D. *Phys. Rev.* **1988**, *A38*, 2398.
(19) Perdew, J. P. *Phys. Rev.* **1986**, *B33*, 8822.
(20) Häser, M.; Almlö, J.; Scuseria, G. E. *Chem. Phys. Lett.* **1991**, *181*, 497.

complexes. In fact, a recent theoretical study has shown that the use of PH_3 ligand in place of aryl- or alkyl-substituted phosphines could lead to significant differences in the geometrical structure of the correponding complexes.[21] The calculated Pd−C bond length has been overestimated by 0.08 Å and is longer than the Pt−C bond, at variance with X-ray data. This is probably due to the neglect of any relativistic effect for Pd. Indeed a previous theoretical study of metal olefin complexes has shown that the inclusion of relativistic effects shortens significantly the Pd−C bond in $Pd(PH_3)_2(C_2H_4)$.[22]

It is noteworthy that the computed M−P bond lengths reproduce fairly well the experimental data for Pd and Pt. The description of the metal phosphorus bond is quite difficult, and previous ab initio calculations at HF levels on the $(PH_3)_2Pt(\eta^2\text{-}C_{60})$ complex led to remarkable deviations of the Pt−P bond length from the experimental value. A deviation of 0.191 Å was calculated by Koga and Morokuma using a 3-21G set for P[12] and was only partially improved to 0.09 Å by Bo et al. through the inclusion of a polarization function on P.[13] We see that the further inclusion of correlation through the DFT approach leads to an excellent agreement of the computed Pt−P bond length with the experimental values, the deviation being only 0.02 Å.

According to the above results, the nickel diphosphine complexes, for which no X-ray structure is yet available, are expected to show a distortion of the C_{60} unit intermediate between those observed for the structurally characterized Pd and Pt complexes.

Bonding Energies. The bond dissociation energies between the C_{60} and $M(PH_3)_2$ fragments, $D(M-C_{60})$, have been calculated according to the following scheme:

$$(PH_3)_2M(\eta^2\text{-}C_{60}) \rightarrow M(PH_3)_2 + C_{60} \qquad (1)$$

where both the fullerene complex and the two fragments have been considered in their ground-state equilibrium geometries. Using the fragment-oriented approach of the DFT computational scheme implemented in the ADF program, the above bond dissociation energies are computed in two steps, as shown in eq 1. First we calculate the "snapping energies", $E^*(M-C_{60})$, i.e., the energies gained when snapping the metal−fullerene bond, obtained by building $(PH_3)_2M(\eta^2\text{-}C_{60})$ from the fragments with the conformation they assume in the equilibrium geometry of the overall complex. In a second step we compute the energies $E^R_{C_{60}}$ and $E^R_{M(PH_3)_2}$ gained when the isolated fragments relax to their equilibrium geometries. This approach also allows the direct computation of the basis set superposition error (BSSE) by applying the counterpoise method.[23] Correction for the zero-point vibrations were not included since they are expected to give small contributions. Baerends et al. have carried out an investigation of the effects of the basis set incompleteness on the bond dissociation energies of some metal−ligand and metal−metal bonds.[24] This work has pointed out that double-ζ plus polarization basis sets give reasonably accurate bond energies for organometallic systems with sufficiently small BSSE corrections to warrant its neglect in most situation.

Table 2. Calculated Bond Dissociation Energies for the $(PH_3)_2M(C_{60})$ and $(PH_3)_2M(C_2X_4)$ Complexes (kJ mol^{-1})

	E^*	BSSE	E^a	$E^R_{M(PH_3)_2}$	$E^R_{C_{60}}$	D
$(PH_3)_2Ni(C_{60})$	255	−34	222	−47	−44	130
$(PH_3)_2Pd(C_{60})$	178	−34	144	−39	−41	63
$(PH_3)_2Pt(C_{60})$	309	−30	279	−130	−40	108
$(PH_3)_2Ni(C_2H_4)$	200	−13	187	−38	−31	118
$(PH_3)_2Pd(C_2H_4)$	124	−9	115	−35	−22	57
$(PH_3)_2Pt(C_2H_4)$	267	−10	253	−121	−57	78
$(PH_3)_2Ni(C_2F_4)$	308	−24	284	−49	−110	125
$(PH_3)_2Pd(C_2F_4)$	209	−22	186	−44	−99	43
$(PH_3)_2Pt(C_2F_4)$	401	−22	379	−141	−149	89
$(PH_3)_2Ni(C_2(CN)_4)$	342	−43	300	−60	−40	199
$(PH_3)_2Pd(C_2(CN)_4)$	253	−44	209	−52	−39	117
$(PH_3)_2Pt(C_2(CN)_4)$	399	−39	360	−145	−75	140

[a] $E = E^* + \text{BSSE}$.

The computational scheme adopted for bonding energies is particularly convenient, as it parallels the most recent convention used to discuss thermochemical data in terms of the two parameters usually considered to measure metal−ligand "bond strengths".[25] According to this convention, reviewed by Martinho Simões and Beauchamp,[25c] the bond dissociation enthalpy, $D(M-L)$, is defined as the enthalpy change of the ligand dissociation process:

$$L'_nM - L \rightarrow L'_nM + L \qquad (2)$$

and is composed of contributions from an "intrinsic" bond enthalpy term $E(M-L)$, the energy required to snap the M−L bond into nonreorganized fragments, and the fragment reorganization energies $E_R(M)$ and $E_R(L)$. Therefore, if we neglect the small thermal correction to enthalpy, we can identify the bond dissociation enthalpy with the calculated bond dissociation energy and the bond enthalpy term with the calculated snapping energies corrected by BSSE.

The results obtained are given in Table 2, where we report all the various contributions, i.e., snapping energies, relaxation energies, and BSSEs. Unfortunately, no experimental data are available for the bond dissociation energy of these metal fullerene complexes, so that no direct comparison is possible. Table 2 shows that the metal−fullerene bond dissociation energy increases in the order Pd < Pt < Ni. Such order for metal−fullerene bond strength within the nickel triad could be surprising with respect to the order observed from geometrical distortion of fullerene complexes (i.e., Pd < Ni < Pt). Indeed, structural data on fullerene complexes deduced from geometrical optimization and confirmed from experimental values indicate a higher degree of distortion of the coordinated fullerene in the platinum complexes, thus suggesting a reversed bond strength order, i.e., Ni < Pt. Table 2 shows that the order of the metal−fullerene bond dissociation energies for the two latter metals (108 and 130 kJ mol^{-1} respectively for Pt and Ni) is determined by the large

(21) Jacobsen, H.; Berke, H. *Chem. Eur. J.* **1997**, *3*, 881. Gonzales-Blanco, O.; Branchadell, V. *Organometallics* **1997**, *16*, 5556.
(22) Li, J.; Schreckenbach, G.; Ziegler, T. *Inorg. Chem.* **1995**, *34*, 3245.
(23) Boys, S. F.; Bernardi, F. *Mol. Phys.* **1970**, *19*, 553.
(24) Rosa, A.; Ehlers, A. W.; Baerends, E. J.; Snijders, J. G.; Velde, G. *J. Phys. Chem.* **1996**, *100*, 5690.
(25) (a) Hartley, F. R. *Chem. Rev.* **1973**, *73*, 27. (b) *Comprehensive Organometallic Chemistry II*; Abel, E. W., Stone, F. G. A., Wilkinson, G., Eds.; Pergamon Press: Oxford, England, 1995; Vol. 9, Chapters 3, 6, and 9. (c) Simões, J. A. M.; Beauchamp, J. L. *Chem. Rev.* **1990**, *90*, 629. (d) Skinner, H. A.; Connor, J. A. *Pure Appl. Chem.* **1985**, *57*, 79.

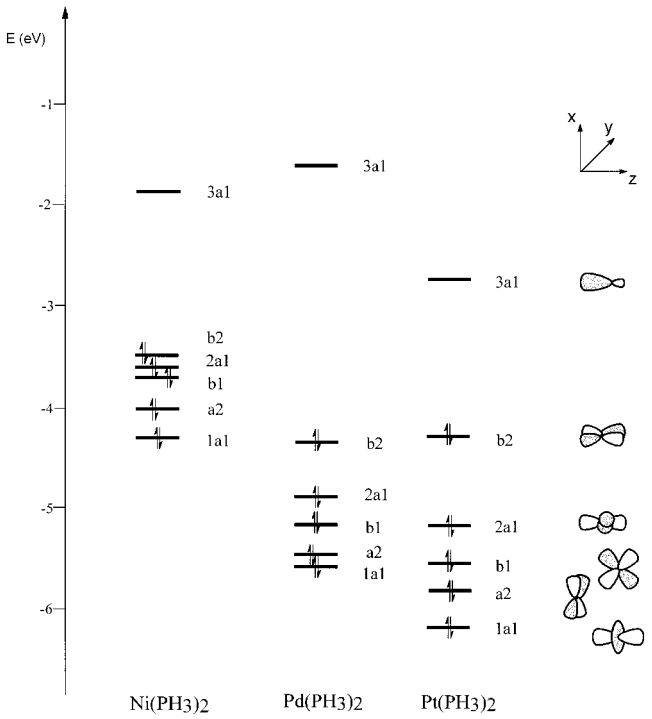

Figure 2. Main valence orbitals of $M(PH_3)_2$ metal fragments.

reorganization energy of the $(PH_3)_2Pt$ fragment (130 kJ mol^{-1}, with respect to 47 kJ mol^{-1} for $(PH_3)_2Ni$), while the order of the bond energy terms is reversed (279 and 222 kJ mol^{-1} respectively for Pt and Ni). Given the similar geometries of $(PH_3)_2Ni$ and $(PH_3)_2Pt$ (see Table 1), this large difference in the reorganization energy seems not to be connected with geometry differences between the two fragments and is probably due to different dependencies of their total energy from the P−M−P angle. On the other hand, the bond energy term seems to be the right thermodynamical parameter to correlate with structural and spectroscopical data, such as bond lengths, bond angles, solid cone angles, and force constants.[25c] This could therefore explain the above discrepancy between the thermodynamical and geometrical data. Such a dichotomy of the thermodynamical and structural data is well documented for the the metal olefin complexes within the nickel triad[25] and has been explained on the basis of the same arguments.[15]

Electronic Structure. The bonding of a side-on coordinated π ligand to a transition metal fragment is usually described by the Dewar−Chatt−Duncanson model.[26] According to this model, the bonding is described in terms of the electron donation from a filled π orbital of the ligand to a suitable vacant metal orbital (σ donation) and of the simultaneous back-donation from an occupied metal d orbital to a vacant π^* orbital of the ligand (π back-donation).

All three considered $M(PH_3)_2$ metal fragments show a LUMO of a_1 symmetry with hybrid $s-p_z$ character and two filled b_1 and b_2 orbitals of d_π character; see Figure 2. C_{60} has many degenerate frontier MOs, whose nodal properties have been already discussed.[27−29] Its molecular orbital diagram is reported in Figure 3 and shows the three highest occupied (h_u, g_g, h_g) and the two lowest unoccupied MOs (t_{1u}, t_{1g}) and their symmetries in both I_h and C_{2v} point groups.

Figure 3 also shows the major interactions between the frontier MOs of C_{60} and those of the $M(PH_3)_2$ fragment. The electron donation into the empty metal σ orbital involves several components of the highest occupied orbitals of C_{60} with π character at the [6,6] C−C bond. The π back-donation involves essentially two components of the t_{1u} and t_{1g} lowest vacant orbitals of C_{60} with π^* character at the [6,6] C−C bond and one of the two d_π orbitals, i.e., the b_2 (d_{yz}) lying in the MC_2 plane.

A Mulliken population analysis in terms of the molecular orbitals of the C_{60} and $M(PH_3)_2$ fragments allows the identification of the orbitals of C_{60} involved in σ donation and π back-donation. The results of such an analysis are reported in Table 3 and shows that the fullerene-to-metal electron donation takes place mainly from three a_1 components of the three highest filled orbitals (h_u, g_u, and h_g) of C_{60} to the $6a_1$ orbital (the LUMO) of the metal fragment. On the other hand, the back-donation from the metal fragment to C_{60} takes place from the metal $4b_2$ (d_{yz}) to two b_2 components of the two lowest t_{1u} and t_{1g} fullerene orbitals.

Table 3. Mulliken Population of the $(PH_3)_2M(C_{60})$ Complexes over the Orbitals of the $M(PH_3)_2$ and C_{60} Fragments

	$M(PH_3)_2$			C_{60}				
	$4a_1$	$6a_1$	$4b_2$	$34a_1$ (h_g)[a]	$36a_1$ (g_g)[a]	$37a_1$ (h_u)[a]	$30b_2$ (t_{1u})[a]	$31b_2$ (t_{1g})[a]
$(PH_3)_2Ni(C_{60})$	1.95	0.12	1.31	1.96	1.96	1.95	0.40	0.15
$(PH_3)_2Pd(C_{60})$	1.92	−0.09	1.39	1.98	1.98	1.97	0.33	0.12
$(PH_3)_2Pt(C_{60})$	1.91	0.16	1.19	1.94	1.93	1.92	0.46	0.18

[a] Orbital symmetries according to the I_h point group of free C_{60}.

To separate the contributions from σ donation and π back-donation, we employed an analysis of the metal−ligand bond dissociation energies based on the extended transition-state method.[30a] The bond dissociation energy is decomposed into a number of contributions:

$$D(M-C_{60}) = -[E_{prep} + E_{ster} + E_{orb}] \qquad (3)$$

The first term, E_{prep}, is the energy necessary to convert the fragments from their equilibrium geometries to the conformation they assume in the optimized structure of the overall complex. Since the fragments have been considered in the same closed shell state both in the complex formation and as free molecules, this term corresponds simply to the sum of the fragment relaxation energies, $E^R_{C_{60}} + E^R_{M(PH_3)_2}$. E_{ster} represents the steric repulsion between the two fragments and consists of two components. The first is the electrostatic interaction of the nuclear charges and the unmodified electronic charge density of one fragment with those of the other fragment. The second component is the so-called Pauli repulsion, which is essentially due to the antisymmetry requirement on the total wave function. E_{orb}, known as the orbital interaction term, represents the attracting orbital interactions that give rise to the energy lowering upon coordination. This term

(26) Dewar, M. J. S. *Bull. Soc. Chim. (Fr.)* **1951**, *18*, C71. Chatt, J.; Ducanson, L. A. *J. Chem. Soc.* **1953**, 2939.
(27) Haddon, R. C.; Brus, L. E.; Raghavachari, K. *Chem. Phys. Lett.* **1986**, *125*, 459.
(28) Haddon, R. C. *Acc. Chem. Res.* **1992**, *25*, 127.
(29) Feng, J.; Li, J.; Wang, Z.; Zerner, M. C. *Int. J. Quantum Chem.* **1990**, *37*, 599.

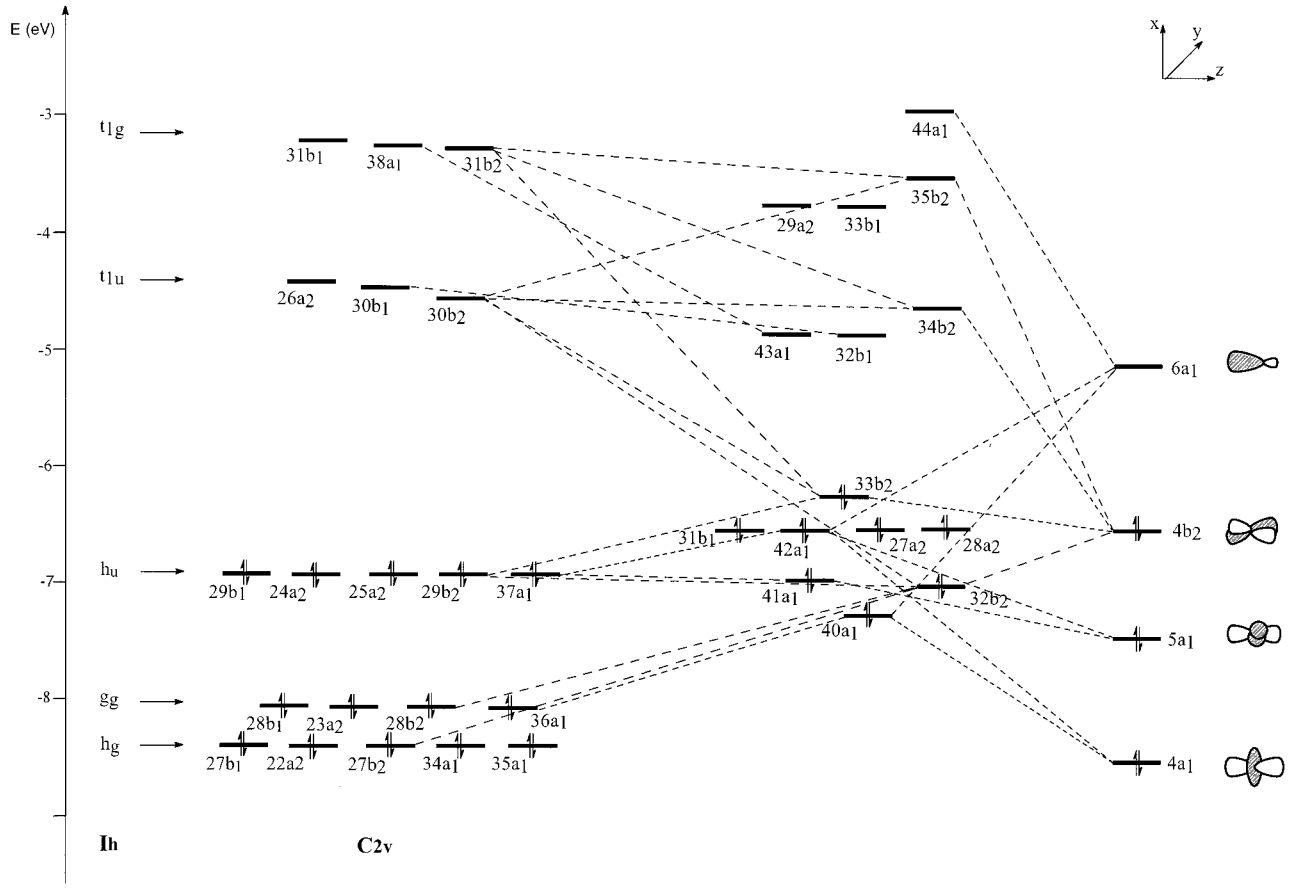

Figure 3. MOs correlation diagram for $(PH_3)_2Pt(\eta^2\text{-}C_{60})$.

Table 4. Bond Dissociation Energy Decomposition for the $(PH_3)_2M(C_{60})$ and $(PH_3)_2M(C_2X_4)$ Complexes (kJ mol^{-1})

	E_{ster}	E_{orb}	E_{A_1}	E_{A_2}	E_{B_1}	E_{B_2}
$(PH_3)_2Ni(C_{60})$	178	−433	−80	−3	−23	−347
$(PH_3)_2Pd(C_{60})$	167	−345	−81	−3	−21	−261
$(PH_3)_2Pt(C_{60})$	287	−596	−168	−7	−34	−410
$(PH_3)_2Ni(C_2H_4)$	102	−305	−71	0	−11	−222
$(PH_3)_2Pd(C_2H_4)$	98	−225	−66	0	−10	−150
$(PH_3)_2Pt(C_2H_4)$	206	−476	−167	−2	−20	−287
$(PH_3)_2Ni(C_2F_4)$	189	−496	−92	−6	−49	−355
$(PH_3)_2Pd(C_2F_4)$	194	−410	−92	−4	−35	−279
$(PH_3)_2Pt(C_2F_4)$	308	−716	−198	−9	−59	−450
$(PH_3)_2Ni(C_2(CN)_4)$	205	−563	−83	−9	−29	−442
$(PH_3)_2Pd(C_2(CN)_4)$	201	−471	−80	−7	−26	−357
$(PH_3)_2Pt(C_2(CN)_4)$	318	−731	−160	−11	−40	−520

may be broken up into contributions from the orbital interactions within the various irreducible representations Γ of the overall symmetry group of the system, according to the decomposition scheme proposed by Ziegler.[30b]

This decomposition scheme is particularly useful in the considered complexes, as it allows one to separate the energy contributions corresponding to σ donation (E_{A_1}) and to π back-donation (E_{B_2}). Indeed, the ligand-to-metal donation takes place into the A_1 representation, while the metal-to-ligand back-donation takes place into the B_2 representation. The results of this energy decomposition for all the considered fullerene complexes are reported in Table 4. It follows from Table 4 that the contribution to the orbital interaction term from π back-donation dominates over that from σ donation.

Table 4 also shows that both σ donation and π back-donation increase in the order Pd, Ni, Pt, showing the same trend calculated for the distortion of the C_{60} unit and indicated by the increase of the C−C bond length and the pyramidalization angle (see Table 1).

Comparison with Substituted Olefins. Buckminsterfullerene shows physical and chemical properties similar to those of electron-deficient alkenes such as tetracyanoethylene (TCNE). For instance, the electron affinity of C_{60}, 2.7 ± 0.1 eV,[33] is very close to that of TCNE, 2.88 eV,[3] and also the C−C bond length in $(PH_3)_2Pt(\eta^2\text{-}C_{60})$, 1.502 Å,[5] is closer to that of the corresponding TCNE complex, 1.490 Å,[31] rather than to that of the ethylene complex, 1.430 Å.[32] It is therefore worth comparing the electronic structure of the considered fullerene complexes with that of ethylene and some substituted ethylenes such as tetrafluoro- and tetracyanoethylene.

In a recent paper we reported NL density functional calculations on $(PH_3)_2M(\eta^2\text{-}C_2X_4)$ ethylene complexes with X = H, F, CN and M = Ni, Pd, Pt to study the effect of electron-attracting substituents on the metal olefin bonding. Optimized energies were obtained in good agreement with the X-ray experimental data.[15]

Bonding energies between the substituted ethylenes and the $M(PH_3)_2$ fragment were also calculated and analyzed with the same approach used above for the full-

(30) (a) Ziegler, T.; Rauk, A. *Theor. Chim. Acta* **1977**, *46*, 1. (b) Ziegler, T. *NATO ASI* **1986**, *C176*, 189.
(31) Bombieri, G.; Forsellini, E.; Panattoni, C.; Graziani, R.; Bandoli, G. *J. Chem. Soc. (A)* **1970**, 1313.
(32) Cheng, P. T.; Nyburg, S. C. *Can. J. Chem.* **1972**, *50*, 912.
(33) Lerke, S. A.; Parkinson, B. A.; Evans, D. H.; Fagan, P. J. *J. Am. Chem. Soc.* **1992**, *114*, 7807.

Table 5. Main Geometrical Parameters for $(PH_3)_2M(C_2X_4)$ Complexes (Bond Lengths in Angstroms and Bond Angles in Degrees)

	$R_{(C-C)}$	$R_{(M-C)}$	δ
$(PH_3)_2Ni(C_2H_4)$	1.403	2.032	18.6
$(PH_3)_2Pd(C_2H_4)$	1.390	2.242	16.0
$(PH_3)_2Pt(C_2H_4)$	1.436	2.097	27.0
$(PH_3)_2Ni(C_2F_4)$	1.418	1.948	32.5
$(PH_3)_2Pd(C_2F_4)$	1.415	2.128	31.9
$(PH_3)_2Pt(C_2F_4)$	1.460	2.043	36.3
$(PH_3)_2Ni(C_2(CN)_4)$	1.469	1.998	19.5
$(PH_3)_2Pd(C_2(CN)_4)$	1.465	2.178	19.4
$(PH_3)_2Pt(C_2(CN)_4)$	1.509	2.043	27.2

erene complexes, and the results were found in reasonable agreement with the available experimental data.

The analysis of the electronic structure in terms of the Chatt−Dewar−Duncanson model showed that (1) the bonding contribution from π back-donation dominates over that from σ donation; (2) the bond energy terms for fluoro- and cyano-substituted ethylene are ca. 60−120 kJ mol^{-1} higher than those for the ethylene complexes and that most of this increase is due to π back-donation, the σ donation remaining almost constant.

Since all calculations of ref 15 were performed with a basis set of triple-ζ plus polarization quality, we reevaluated equilibrium geometries and bonding energies using the same double-ζ plus polarization basis set employed in this work. Indeed the results were found very close to those of ref 15. The comparison between the calculated thermodynamical parameters for fullerene and C_2X_4 complexes (see Table 2) shows that the bond energy terms for C_{60} are ca. 20−40 kJ mol^{-1} higher than those of ethylene complexes and ca. 40−100 kJ mol^{-1} lower than those of substituted ethylene complexes, C_2F_4 and $C_2(CN)_4$. This result agrees with the experimental evidence showing for the coordinated tetrafluoro- and tetracyanoethylene a longer C−C bond length and a larger pyramidalization angle (see Tables 1 and 5) with respect to buckminsterfullerene and ethylene. A less clear trend is observed for the bond dissociation energies, due to the different reorganization energies of the organic fragments. There is an evident increase of ca. 10−30 kJ mol^{-1} from ethylene to fullerene and of ca. 30−70 kJ mol^{-1} from fullerene to tetracyanoethylene complexes; on the other hand the bond dissociation energies decrease 5−20 kJ mol^{-1} passing from fullerene to tetrafluoroethylene.

The values reported in Table 4 indicate that the symmetry decompositions of the binding energies for C_{60} complexes are qualitatively similar to those calculated for the electron-deficient alkene complexes C_2F_4 and $C_2(CN)_4$. Indeed, most of the increase calculated for the bond energy terms on passing from ethylene to fullerene (ca. 20−40 kJ mol^{-1}) or from ethylene to substituted olefins (ca. 60−120 kJ mol^{-1}) is due mainly to the π back-donation contribution, the σ contribution remaining almost constant. This can be explained by taking into account that C_{60}, C_2F_4, and $C_2(CN)_4$ have a higher electron affinity than ethylene, while the ionization energies are comparable.

Electrochemistry of Metal Transition Fullerene Complexes. The electrochemical properties of the complexes $(PPh_3)_2Pt(\eta^2\text{-}C_{60})$ and $(PEt_3)_2M(\eta^2\text{-}C_{60})$ (M = Ni, Pd, Pt) have been recently investigated.[33,34] Cyclic voltammetry of these complexes reveals three reversible fullerene-based reduction waves, which have been assigned to the formation of $[(PR_3)_2M(C_{60})]^-$, $[(PR_3)_2M(C_{60})]^{2-}$, and $[(PR_3)_2M(C_{60})]^{3-}$. The reduction potentials are shifted by ca. 0.32−0.34 V to more negative values than those of C_{60} and are essentially independent of the nature of the metal; see Table 6. Moreover, the increase of free C_{60} concentration as the $(PR_3)_2M(C_{60})$ solutions are cycled through the reduction process indicates that the metal−fullerene binding energy decreases upon reduction. In particular, a kinetic simulation of the voltammograms has shown that the loss of C_{60}^- from the $[(PR_3)_2M(C_{60})]^-$ anions is ca. 31−33 kJ mol^{-1} more favorable than the loss of C_{60} from the corresponding neutral complexes.

Table 6. Calculated Gas-Phase Electron Affinities Differences ($\Delta(EA_{calc})$, eV), First Reduction Potential Shifts ($\Delta\epsilon^\circ_{calc}$, V), and Experimental First Reduction Potential Shifts ($\Delta\epsilon^\circ_{exp}$, V) for $(PH_3)_2M(C_{60})$ Complexes

	$\Delta(EA_{calc})$	$\Delta\epsilon^\circ_{calc}$ [a]	$\Delta\epsilon^\circ_{exp}$ [b]
C_{60}	0.00	0.00	0.00
$(PH_3)_2Ni(C_{60})$	−0.37	−0.34	−0.34
$(PH_3)_2Pd(C_{60})$	−0.40	−0.37	−0.32
$(PH_3)_2Pt(C_{60})$	−0.39	−0.36	−0.34

[a] See text. [b] Reference 32.

To elucidate the nature of the first reversible reduction of fullerene complexes, we have performed density functional calculations on the $[(PH_3)_2M(\eta^2\text{-}C_{60})]^-$ anions. Geometry optimizations have been carried out to evaluate the effect of reduction on the geometry and bonding energy of the considered complexes.

We first calculated vertical electron affinity (EA) for C_{60} and the three fullerene complexes, and the results are shown in Table 6. Our calculations give for C_{60} an electron affinity of 3.5 eV, which, despite the relatively poor basis set, is qualitatively consistent with the experimental value of 2.7 ± 0.1 eV.[33] For instance, UHF calculations with a similar basis set led to an unrealistic value of 0.87 eV.[35] Table 6 illustrates that upon metal binding, the EA of fullerene is reduced by ca. 0.37−0.40 eV. Although no experimental data are available for the gas-phase EA of these fullerene complexes, it is worth comparing our calculations with the shift of reduction potentials experimentally observed for these complexes. Our comparison is based on the experimental evidence that solution-phase redox potentials are often found to correlate linearly with gas-phase electron affinities.[36] Slopes, d(ϵ°)/d(EA), close to unity have been usually found, such as 0.92 V/eV in ref 37. Assuming a linear relationship between ϵ° and EA with a slope of 0.92, the shifts of reduction potentials calculated for the metal fullerene complexes should fall in the range 0.34−0.37 V, in excellent agreement with the experimental data; see Table 6.

The results of the geometrical optimizations show that the reduction affects only slightly the geometrical

(34) Chernega, A. N.; Green, M. L. H.; Haggitt, J.; Stephens, A. H. H. *J. Chem. Soc., Dalton Trans.* **1998**, 755.
(35) Koga, N.; Morokuma, K. *Chem. Phys. Lett.* **1992**, *196*, 191.
(36) Shalev, H.; Evans, D. H. *J. Am. Chem. Soc.* **1989**, *111*, 2667, and references therein.
(37) Dewar, M. J. S.; Hashmall, J. A.; Trinajstić, N. *J. Am. Chem. Soc.* **1970**, *92*, 5555.

Table 7. Main Optimized Parameters, Bond Dissociation Energies, and Bond Energy Decomposition for the $(PH_3)_2M(C_{60})^-$ Anions[a]

	$(PH_3)_2Ni(C_{60})^-$	$(PH_3)_2Pd(C_{60})^-$	$(PH_3)_2Pt(C_{60})^-$
$R_{([6,6])}$	1.463	1.453	1.493
$R_{(M-C)}$	2.015	2.189	2.110
δ	38.0	37.2	39.9
E^*	212	136	251
BSSE	−30	−30	−26
E^b	182	106	225
$E^R_{M(PH_3)_2}$	−46	−42	−126
$E^R_{C_{60}}$	−22	−20	−36
D	114	44	63
E_{A_1}	−75	−79	−175
E_{A_2}	0	0	−4
E_{B_1}	−21	−21	−33
E_{B_2}	−297	−226	−364

[a] Bond lengths in angstroms and bond angles in degrees; energies in kJ mol^{-1}. [b] $E = E^* +$ BSSE.

parameters of the interaction region, as expected since the additional electron occupies a C_{60}-based molecular orbital. However, we found that the anions are less stable than the corresponding neutral complexes. Indeed we calculated the bond dissociation energies between C_{60}^- and the $M(PH_3)_2$ fragments, using the same scheme seen for the neutral complexes, and the results are reported in Table 7. The bond energies calculated for the anions are 16−44 kJ mol^{-1} lower than those for the neutral complexes, in agreement with the experimental evidence of 31−33 kJ mol^{-1} (see above).

The results of the bond energy symmetry decomposition in Table 7 show that this decrease is essentially due to the π back-donation contribution, of B_2 symmetry (E_{B_2}), while the σ donation contribution (E_{A_1}) remains almost constant. This analysis shows therefore that the presence of an additional electron on the C_{60} inhibits back-donation from the metal fragment.

4. Conclusions

We have performed density functional calculations on the $(PH_3)_2M(\eta^2\text{-}C_{60})$ complexes for the group 10 metals Ni, Pd, and Pt at the DFT nonlocal level, using polarized basis sets for P, C, and H. The optimized geometries are found in good agreement with the X-ray experimental data. The electronic structure is analyzed in terms of the Chatt−Dewar−Duncanson model, and the contribution from π back-donation dominates over that from σ donation for all three complexes. Reliable values for the metal fullerene bond dissociation energies have been calculated. The bond dissociation energies computed for the fullerene complexes increase in the order Pd < Pt < Ni. Bond dissociation energies have been analyzed in terms of "intrinsic" bond energy terms and fragment reorganization energies and allowed us to give a rationale for the dichotomy between thermochemical and structural data on the metal ethylene bond strength, within the nickel triad. The calculated bond energy terms increase in the order Pd < Ni < Pt, showing the same trend observed for the distortion of the C_{60} unit, as indicated by the increase of the C−C bond length and the pyramidalization angle. DFT calculations were also performed for some related $(PH_3)_2M(\eta^2\text{-}C_2X_4)$ (X = CN, F) substituted ethylene complexes to compare electronic structure and bond energies. This comparison has shown that the bond energy terms for fullerene complexes are ca. 20−40 kJ mol^{-1} higher than for the ethylene complexes and ca. 40−100 kJ mol^{-1} lower than those of substituted ethylene complexes,while no clear trend is observed for the bond dissociation energies because of large reorganization energy effects.

Acknowledgment. The present work has been carried out in the context of the COST D9 Action. Thanks are due to CNR (Progetto Finalizzato "Materiali Speciali per Tecnologie Avanzate II") for financial support.

OM9908478